# Design and functional test of a novel optical testing target*

**ZHANG Shao-jun** (张绍军)[1,2]**, **GAO Yun-guo** (高云国)[1], **XUE Xiang-yao** (薛向尧)[1], **WANG Guang** (王光)[1], **and LI Heng-dong** (李恒东)[3]

*1. Changchun Institute of Optics, Fine Mechanics and Physics, Chinese Academy of Science, Changchun 130033, China*

*2. University of Chinese Academy of Science, Beijing 101408, China*

*3.China Petroleum Pipeline Engineering Co., Ltd, Langfang 065000, China*

(Received 30 March 2018; Revised 7 June 2018)



A novel optical testing target (OTT) with three degrees of freedom (DOFs) is proposed for measuring the tracking performance of a photoelectric theodolite. The main components, such as the azimuth axis system, the pitching axis system, the linear motion system, and the simulated target generator, are designed. Furthermore, the linear module with the form of a large-span and low-stiffness cantilever beam is strengthened using an integrated optimization method. After the structure is strengthened, the 1st-order natural frequency increases from 14 Hz to 32 Hz. Finally, a functional test is performed and the results show that compared with a traditional optical test target, the simulated target generated by the novel target is advantageous in practice.

**Document code:** A **Article ID:** 1673-1905(2018)06-0461-4

**DOI** https://doi.org/10.1007/s11801-018-8061-6

The optical testing target (OTT) is a special type of testing equipment. It is designed for indoor measurement of the technical performance of photoelectric theodolites. Therefore, the OTT plays a crucial role in the development of photoelectric theodolites. Currently, OTTs in assembly workshops are mainly divided into two categories: the static test target and the dynamic test target. The former is also called a stationary test frame, as shown in Fig.1(a). The latter is divided into the test target with a single degree of freedom (DOF) and that with two DOFs[1]. Fig.1(b) shows the OTT with a single DOF. The existing OTT has disadvantages in the performance testing of large-scale photoelectric theodolites. Researchers have revealed that there are defects in the motion characteristics of the simulation target provided by the OTT with a single DOF[3]. For example, the trajectory of the simulated target is single, the range of motion is small, and the movement speed and acceleration cannot be arbitrarily set.

In this study, to adapt to the development of the photoelectric theodolite, a new test method is proposed, and a novel OTT with three DOFs is designed. As shown in Fig.2, it consists of a braced frame, an azimuth axis system, a linear motion system, a pitching axis system and a collimator. When the equipment is working, the azimuth axis system can drive the linear motion system to rotate $n$×360º in the azimuth direction. The linear motion system can drive the pitching axis system to move along the linear guide rail. The pitching system can drive the collimator to rotate within the pitch-angle range from 30º to 65º.

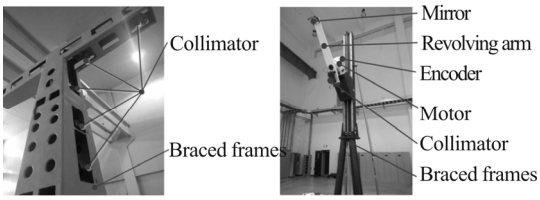


**Fig.1 Traditional OTT**

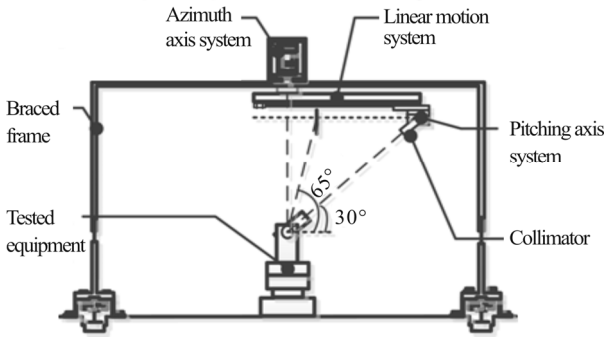


**Fig.2 Schematic of the novel OTT**

* This work has been supported by the Third Phase of the Innovation Project Funding of Changchun Institute of Optics, Fine Mechanics and Physics, Chinese Academy of Science (No.061X20C060).

** E-mail: zhangsj198609@126.com

In general, the design of precision shafting involves relatively mature technology. The design of a common two-axis supporting turntable was previously reported[5]. However, owing to the different spatial layouts of the shaft structure, the shaft structure of the common biaxial supporting turntable is not entirely suitable for the azimuth and pitching axis systems of the novel OTT. As shown in Fig.2, the layout of the azimuth axis system is located above the pitching axis system and causes high stress and deformation of the azimuth shaft. Therefore, finite-element analysis (FEA) of the self-designed hollow shafts is performed. As shown in Fig.3, the analysis results indicate that the maximum stress and deformation are no more than 3.0 MPa and $1.5\times10^{-3}$ mm, respectively. According to the deformation amount, the maximum torsion angles can be calculated as approximately $2.0\times10^{-3}$° and $1.0\times10^{-5}$°, respectively. The remaining accessories of the two shafting systems include precision bearings, absolute encoders[7] and conductive rings. Considering that the shaft is subject to both axial and radial forces, the bearings selected are angular contact ball bearings from FAG Company (B71930C.T.P4S.UL, B7008C.T.P4 S.UL, Germany). The bearings are mounted face to face. Similarly, according to the tracking-accuracy requirements of the tested equipment, an absolute encoder with an angular resolution of 1.5° from HEIDENHAIN is installed on each shaft (ECN113, Germany). They are used as the angle sensors for the electric control system of the azimuth axis or the pitching axis. In addition, the signal and driving currents of the revolute components are exchanged with external static equipment through a conductive ring.

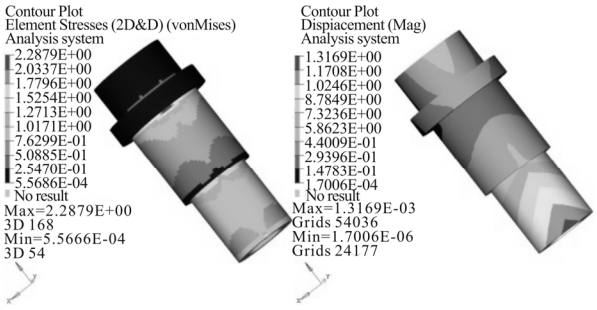


(a) Hollow shaft in azimuth axis system

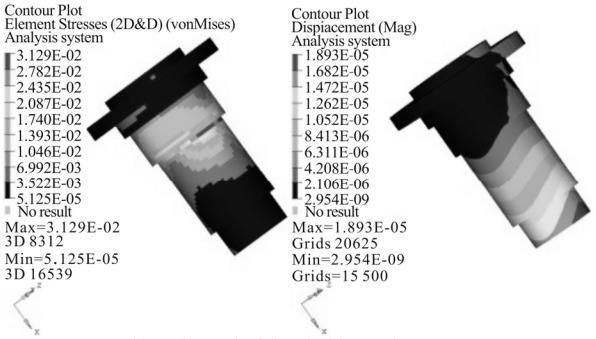


(b) Hollow shaft in pitching axis system

**Fig.3 FEA of the shaft**

The linear motion system shown in Fig.4 is a horizontal drive component. It is mainly composed of a motor, a linear module[9], a slider, a reinforcing beam and reinforcing plates. The motor drives the synchronous-belt movement through a gear reducer with a reduced ratio of 8, so that the rotational movement of the motor is converted into the linear movement of the slider. The motor is from Phase Company (PH506, Italy), and the synchronous belt is from the Berger Lahr Company (MLZ100, Germany). The linear module has a total length of 3 m and is installed in the form of a cantilever beam. However, owing to the low stiffness of the cantilever structure, it is difficult to satisfy the stiffness requirements of the linear motion system. Therefore, it is necessary to strengthen the linear module by using a reinforcing beam and reinforcing plates to increase the rigidity of the structure. Thus, structural integrated optimization techniques are adopted. The FEA and structural vibration experiment verify that the first-order natural frequency of the horizontal motion system increases from 14 Hz to 32 Hz[10].

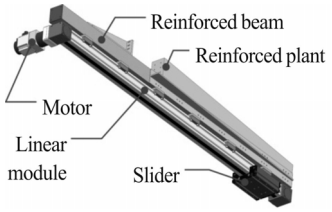


**Fig.4 Assembly diagram of the linear motion system**

Collimators are commonly used as inspection equipment. Their optical system structure is based on a reflective or refractive optical system. The reflective collimator is superior to the refractive collimator in which the working wavelength range can be adjusted by changing the coating of the mirror, and the emitted collimated beam has no chromatic aberration. Therefore, the former is more popular in practical applications. Here, a Cassegrain-type collimator is selected as the simulated target generator of the novel OTT[11]. It is a typical reflective optical system, as shown in Fig.5(a). It is mainly composed of an iodine-tungsten lamp, a primary mirror, a secondary mirror, a star tester and a laser, as shown in Fig.5(b). Among these, the iodine-tungsten lamp used for illumination mainly radiates visible and infrared light. The diameter of the concave paraboloid primary mirror is 100 mm, the diameter of the central hole is 18 mm, and the diameter of the convex hyperboloid secondary mirror is 25 mm. The bases of both mirrors are made of K9 optical glass, and their coefficient of thermal expansion is close to zero. For adequate accuracy of the surface shape of the primary and secondary mirrors, the root-mean-square error must be less than 1/15 and 1/30 of the red wavelength, respectively, which ensures the parallelism of the outgoing beam. The focal length of the optical system is 1 000±5 mm. A star tester with 0.02-mm-diameter star holes is installed on the focal plane. When the light emitted by the iodine-tungsten lamp

uniformly illuminates the star tester, the star-hole pattern is imaged on the charge-coupled device of the tested equipment. In addition, a coaxially mounted laser is used as an indicator to facilitate the placement of the tested equipment.

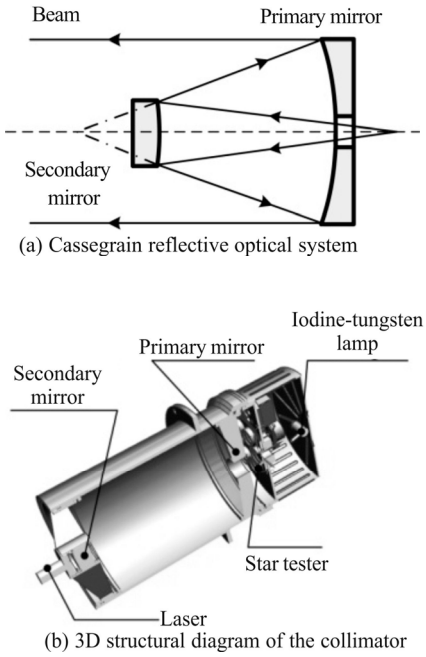


**Fig.5 Structure of the collimator**

A 3D assembly diagram of the entire novel OTT is shown in Fig.6. In addition to the aforementioned components, a braced frame serves as the base.

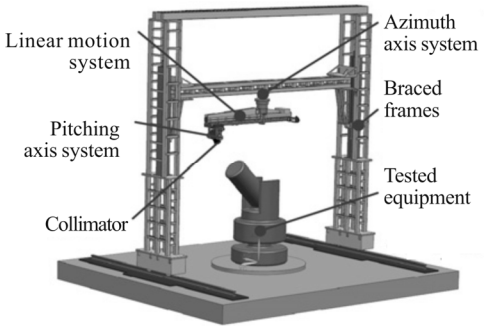


**Fig.6 Assembly model view of the novel OTT**

Experiments were conducted using the conventional OTT with a single DOF and the novel OTT. Before the start of the testing, it was necessary to ensure that the intersection of laser-aided marking line coincided with the intersection of the three axes of the photoelectric theodolite, as shown in Fig.7. The specific values of the related parameters in the experiments are shown in Tab.1[3]. The tester inputs the required motion control parameters $\theta$ or $A$ and $E$ to the industrial control computer (ICC), and then the motion control card receives the information from the ICC and the encoder feedbacks and sends the command to control the motor drive shafting. Through the exchange of signals between multiple components, the ICC can display the motion parameters of each axis in real time. Simultaneously, the infrared detector of the photoelectric theodolite captures the simulated target generated by the collimator[14]. The tracking data were recorded by the recording device at a frequency of 50 Hz.

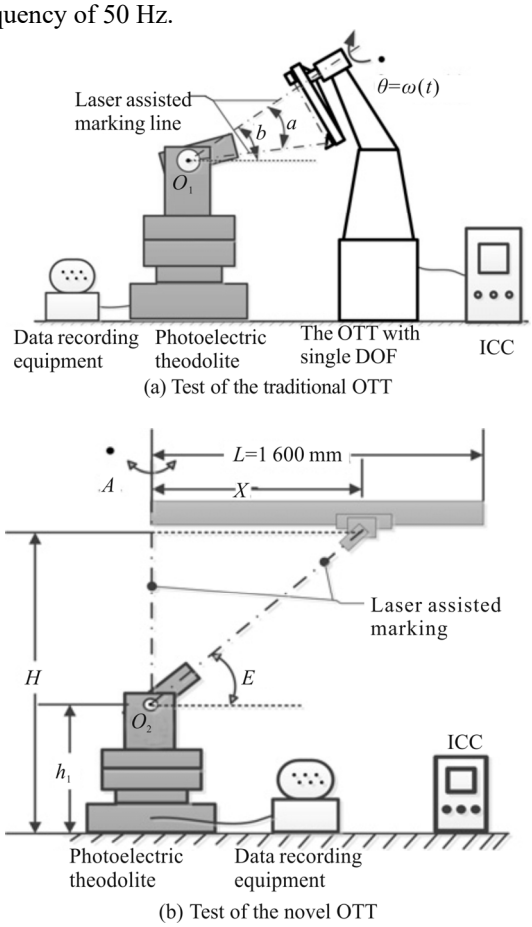


**Fig.7 Spatial layout between the OTT and the photoelectric theodolite**

**Tab.1 Parameters used in the experiment**

| Parameter | Value | Parameter | Value |
|---|---|---|---|
| $a$ | 33.5° | $L$ | 1 600 mm |
| $b$ | 23.5° | $E$ | 55.19° |
| $H$ | 3 840 mm | $x$ | 1 438 mm |
| $h_1$ | 1 700 mm | | |

The test results are shown in Fig.8, indicating that the traditional OTT can only generate a simulated target with a single trajectory, a 30° range of azimuth motion, a 23° range of pitch angle motion, and a unique velocity profile. Because the angle velocity and acceleration are related in real time, it is not easy to match the tracking target with the specific angle velocity and angle acceleration required by a photoelectric theodolite. However, as shown in Fig.9, the novel OTT can generate simulated targets with different trajectories, an $n\times360^{\circ}$ range of azimuth motion, and various velocity patterns. The angle velocity and angle acceleration of such targets can be arbitrarily matched to satisfy the requirements of any photoelectric theodolite. For example, when tracking the simulated target with a 25°/s azimuth angle velocity and a 15°/s$^2$

azimuth angle acceleration, the tracking technical index of the tested photoelectric theodolite is that the miss distance is no greater than 25 detector pixels[15]. The azimuthal velocity of the simulated target generated by the traditional OTT is 15°/s, and the angular acceleration reaches 30°/s$^2$. With the novel OTT, it is easy to generate the desired simulated target.

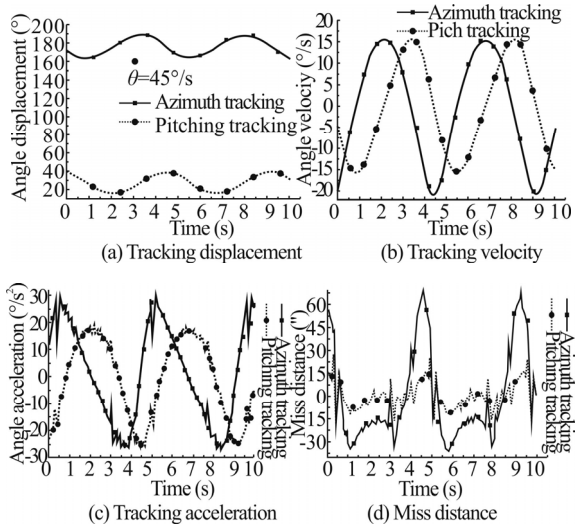


**Fig.8 Tracking response of the traditional OTT with a single DOF**

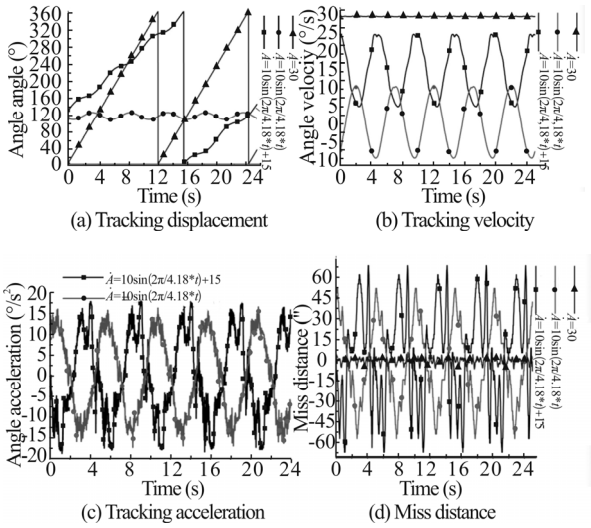


**Fig.9 Azimuth tracking response of the novel OTT**

In summary, a novel OTT is proposed. The design of its main components is introduced. In the azimuth axis system and the pitching axis system, the self-designed shafts have a small amount of torsional deformation and can satisfy the requirement of the torsional stiffness. The linear module with a large-span and low-stiffness in the linear motion system is strengthened, increasing its first-order natural frequency from 14 Hz to 32 Hz. The Cassegrain collimator is selected as the target generator, and its technical requirements are determined. In addition, the standard parts of each component are determined, such as encoders, torque motors, and conductive rings. Finally, a functional experiment involving the novel OTT is performed. The results show that the designs of the optical system, the mechanism, and electronic control system are feasible. Compared with the simulated target generated by the traditional OTT with a single DOF, the simulated target generated by the novel OTT has the advantages of flexible matching between the angle velocity and angle acceleration, a wide range of motion, and various movement trajectories.

## References

[1] Min Gao, Zhenglan Bian, Zuoren Dong, Qing Ye and Ronghui Qu, Proc. SPIE **7654**, 76540C (2010).

[2] Liu Manlin, Hao Bin, Cao Yan and XIONG Rensheng, Optical Technique **35**, 815 (2009). (in Chinese)

[3] Gu Yinying, Shen Xiangheng and HE Genxian, Optoelectronic Engineering **3**, 19 (2011). (in Chinese)

[4] Miao Li and Huibin GAO, Advanced Materials Research **472**, 1383 (2012).

[5] Xu Han, Ming Liu, Jun Ma, Sheng Li and Jia Liu, Proc. SPIE **10255**, 102550O-1 (2017).

[6] Nian Cai, Wei Xie, Hongxia Peng, Han Wang, Zhijing Yang and Xin Chen, Mechanical Systems and Signal Processing **88**, 81 (2017).

[7] CHEN Yun, Optoelectronics Letters **3**, 78 (2007).

[8] Subir Das, Sensors Journal **16**, 2300 (2016).

[9] ZHAO Y X, SHEN M D and CUI Y B, Advanced Materials Research **694**, 3151 (2013).

[10] ZHANG Shaojun, GAO Yunguo and XUE Xiangyao, Infrared and Laser Engineering **47**, 1512 (2018). (in Chinese)

[11] Mustafa Ekinci and Özgür Selimoğlu, Advances in Optical and Mechanical Technologies for Telescopes and Instrumentation II **9912**, 53 (2016).

[12] Yang Juqing, Wang Dayong and Zhou Weihu, Optik **131**, 994 (2017).

[13] Ruijuan Guo, Shuang Du and Huimin Yin, 10th International Congress on Image and Signal Processing, BioMedical Engineering and Informatics (CISP-BMEI 2017) **978**, 5386 (2017).

[14] Hai-ying Wu, San-xi Zhang, Biao Liu, Peng Yue and Ying-hui Weng, Proc. SPIE **10697**, 1069716 (2018).

[15] Yong-qing Yang, Peng Liu, Wen-ji Shen and Jun-feng Han, Proc. SPIE **10697**, 106975K-1 (2018).

[16] XIAO Wen-jian, CHEN Zhi-bin, MA, Dong-xi, ZHANG Yong, LIN Xian-hong and QIN Meng-ze, Optoelectronics Letters **12**, 229 (2016).